Increased atherosclerosis in myeloperoxidase-deficient mice

Marie-Luise Brennan,[1] Melissa M. Anderson,[2] Diana M. Shih,[3] Xiao-Dan Qu,[3]
Xuping Wang,[3] Asha C. Mehta,[3] Lesley L. Lim,[3] Weibin Shi,[3] Stanley L. Hazen,[4]
Jason S. Jacob,[2] Jan R. Crowley,[2] Jay W. Heinecke,[2] and Aldons J. Lusis[1,3,5]

[1]Department of Microbiology, Immunology and Molecular Genetics, University of California,
 Los Angeles (UCLA), Los Angeles, California, USA
[2]Departments of Medicine and Molecular Biology and Pharmacology, Washington University, St. Louis, Missouri, USA
[3]Department of Medicine, UCLA, Los Angeles, California, USA
[4]Departments of Cardiology and Cell Biology, Cleveland Clinic Foundation, Cleveland, Ohio, USA
[5]Department of Human Genetics, UCLA, Los Angeles, California, USA

Address correspondence to: Aldons J. Lusis, UCLA, Department of Medicine, 47-123 Center for Health Sciences,
Los Angeles, California 90095-1679, USA. Phone: (310) 825-1359; Fax: (310) 794-7345; E-mail: jlusis@mednet.ucla.edu.

Marie-Luise Brennan's present address is: Cleveland Clinic Foundation, Department of Cell Biology, Cleveland, Ohio, USA

Myeloperoxidase (MPO), a heme enzyme secreted by activated phagocytes, generates an array of oxidants proposed to play critical roles in host defense and local tissue damage. Both MPO and its reaction products are present in human atherosclerotic plaque, and it has been proposed that MPO oxidatively modifies targets in the artery wall. We have now generated MPO-deficient mice, and show here that neutrophils from homozygous mutants lack peroxidase and chlorination activity in vitro and fail to generate chlorotyrosine or to kill *Candida albicans* in vivo. To examine the potential role of MPO in atherosclerosis, we subjected LDL receptor–deficient mice to lethal irradiation, repopulated their marrow with MPO-deficient or wild-type cells, and provided them a high-fat, high-cholesterol diet for 14 weeks. White cell counts and plasma lipoprotein profiles were similar between the two groups at sacrifice. Cross-sectional analysis of the aorta indicated that lesions in MPO-deficient mice were about 50% larger than controls. Similar results were obtained in a genetic cross with LDL receptor–deficient mice. In contrast to advanced human atherosclerotic lesions, the chlorotyrosine content of aortic lesions from wild-type as well as MPO-deficient mice was essentially undetectable. These data suggest an unexpected, protective role for MPO-generated reactive intermediates in murine atherosclerosis. They also identify an important distinction between murine and human atherosclerosis with regard to the potential involvement of MPO in protein oxidation.

J. Clin. Invest. **107**:419–430 (2001).

Introduction

Phagocytic white blood cells are important in host defense and may inflict oxidative damage during inflammation (1–4). One key component of their cytotoxic armamentarium is myeloperoxidase (MPO), a heme enzyme that localizes to azurophilic granules. MPO constitutes approximately 5% of human neutrophil protein (5) and approximately 1% of monocyte protein (6), and recent studies suggest it is also present in certain tissue macrophages (7, 8). When neutrophils ingest bacteria and fungi or are otherwise activated, they secrete large quantities of MPO and produce superoxide in the phagolysosome and the extracellular compartment. The superoxide dismutates to hydrogen peroxide (H_2O_2), a relatively unreactive oxidant; MPO then uses peroxide as a substrate to form hypochlorous acid (HOCl): $H_2O_2 + Cl^- + H^+ \rightarrow HOCl + H_2O$.

At plasma concentrations of halide ion, HOCl is a major oxidant generated by the heme enzyme (9, 10), and MPO is the only human enzyme known to generate HOCl under these conditions (11). HOCl is a potent bactericidal and viricidal agent in vitro (12, 13) and reacts readily with biomolecules containing nucleophilic and other electron-rich moieties, presumably oxidizing key functional components of ingested microorganisms.

MPO deficiency is a relatively common genetic defect that occurs at a frequency of 1 in every 2,000 to 4,000 Caucasians, and the responsible mutations are not yet fully characterized (reviewed in refs. 14, 15). MPO-deficient neutrophils are normal in terms of chemotaxis and phagocytosis, but display impaired candidacidal activity (16) and delayed bacterial killing in vitro (17). Although MPO is an efficient germicidal agent and amplifies the toxic potential of neutrophil-generated oxidants, most MPO-deficient humans do

not exhibit recurrent bacterial or fungal infections (14). Cases of overwhelming *Candida* sepsis have been reported, but the majority of those individuals also possessed immune-compromising conditions such as diabetes mellitus (14).

In addition to their role in host defense, reactive intermediates generated by MPO may damage host tissue at inflammatory foci (18–20). Oxidative products characteristic of MPO have been observed in diseased tissue (21–24), and genetic association studies have suggested its involvement in various pathophysiological processes (8, 25–28). There are several pathways through which MPO could damage biological targets, and all require H_2O_2 and a low-molecular-weight intermediate, such as chloride, tyrosine, or nitrite. One potential pathway is through generation of HOCl, which can modify both lipids and proteins (22, 29–36). Another pathway is via tyrosyl radical, which is generated from free plasma L-tyrosine (37) and is capable of initiating lipid peroxidation (38) and cross-linking tyrosine residues on proteins (39). A third pathway is through oxidation of nitrite, a decomposition product of nitric oxide, to generate nitrating and possibly chlorinating intermediates (40–43) and to initiate lipid oxidation (43, 44).

Atherosclerosis, the major cause of heart disease and stroke, is a chronic inflammatory disease in which monocytes play a key role and in which lipid and protein oxidation appear to be involved (reviewed in refs. 45–47). Oxidative modification to LDL is thought to contribute to the accumulation of cholesterol-loaded macrophages, termed "foam cells", that are a hallmark of the disease (45–47). Catalytically active MPO is present in human atherosclerotic tissue, where it colocalizes with foam cells (7). Moreover, elevated levels of chlorinated, tyrosylated, and nitrated proteins that may result from MPO-mediated reactions have been detected in atherosclerotic tissue (22, 48–50). Specific mass-spectrometric assays have detected 30-fold increased levels of chlorotyrosine (22), 100-fold increased levels of dityrosine (48), and 90-fold increased levels of nitrotyrosine (50) in LDL from atherosclerotic lesions as compared with circulating LDL. Exposure of LDL to bolus addition of reagent HOCl (51) or the MPO-H_2O_2-nitrite system of monocytes (43) converts the lipoprotein into a high-uptake form, the former through phagocytosis of aggregated oxidized lipoprotein (43, 52), the latter by recognition by the macrophage scavenger receptor CD36 (53). These results provide evidence that reactive intermediates formed by MPO serve as a pathway for oxidizing lipids and proteins in vivo and may be critical in rendering LDL atherogenic.

We now report studies with MPO-deficient mice, created by gene targeting, to examine the role of MPO in the generation of reactive oxidants, its role in host defense, and its involvement in atherosclerosis. During the preparation of this manuscript, Aratani et al. (54) reported studies with MPO-deficient mice that addressed issues relating to host defense. Our model showed similar inability to kill fungi, but also revealed that MPO serves an unexpected, protective function in atherosclerosis in a hypercholesterolemic murine model.

Methods

Genomic cloning and construction of the targeting vector. A 5.8-kb *MPO* gene fragment was amplified from mouse 129/SvJ DNA using Long and Accurate PCR (Takara Shuzo Co., Shiga, Japan). Primers were designed to anneal starting at position 228 in the 5′ untranslated region and at position 5993 in intron 8 of the BALB/c sequence (55). The resulting PCR product was isolated and cloned into a pGEM-T-Vector (Promega Corp., Madison, Wisconsin, USA) using standard procedures. Clone identity was verified by sequencing and by Southern blot hybridization using a human MPO cDNA (56) kindly provided by H. P. Koeffler and C. Miller (UCLA) as a probe. The pNTK plasmid, containing a PGK-neomycin resistance (PGK-Neo) expression cassette and a HSV-thymidine kinase (HSV-TK) expression cassette, was selected as a parental plasmid for targeting vector construction. Restriction analysis of the genomic *MPO* clone indicated a unique *Bss*HII restriction enzyme site in exon 7. Digestion at this site was performed in conjunction with either *Sac*II or *Not*I digestion to generate a 3.7-kb 5′ portion or a 2.1-kb 3′ portion of the *MPO* gene. *Cla*I linkers were added to the 5′ fragment, and *Bam*HI linkers were added to the 3′ portion. The 5′ fragment was cloned into the *Cla*I site of the pNTK plasmid upstream of PGK-Neo, while the 3′ fragment was inserted into a *Bam*HI site flanked by PGK-Neo and HSV-TK. The resulting *MPO* targeting vector was CsCl purified and linearized using *Sal*I.

Gene targeting and generation of mutant mice. RW4 embryonic stem cells (from strain 129/SvJ) were purchased from Genome Systems Inc. (St. Louis, Missouri, USA) and neomycin-resistant murine fibroblasts were kindly provided by K. M. Lyons (UCLA). Embryonic stem cells were cultured following manufacturer's instructions, and a total of eight separate electroporations were performed using 25 μg of DNA and 10^7 cells each time. Embryonic stem cells resistant to both ganciclovir (2 μM; Syntex, Palo Alto, California, USA) and G418 (200 μg/ml; Life Technologies Inc., Rockville, Maryland, USA) were expanded. DNA was isolated, digested with *Bgl*II, and screened using Southern blot hybridization with an intron 8 probe. Cells targeted in the *MPO* locus were injected into blastocysts, implanted into pseudopregnant Swiss Webster mice, and chimeric animals were obtained. The chimeric mice were bred to strain C57BL/6J mice, and mice carrying the mutant *MPO* allele were crossed to C57BL/6J mice for two or more generations to reduce genetic variation. Host defense and protein oxidation experiments described in this paper used age- and sex-matched wild-type and mutant animals from intercrosses of heterozygous (*MPO*+/−) mice. Genetic composition of mice used for atherosclerosis studies is described below.

Northern and Western blot analyses and peroxidase-activity staining. Bone marrow cells were flushed from mouse femurs and RNA isolated using Trizol reagent (Life Technologies Inc.). Samples were run on a 1% agarose formaldehyde gel, transferred to nylon membrane, and probed with a complete human cDNA probe (56). For Western blot analyses, aortae and bone marrow cells were solubilized with lysis buffer (10 mM Tris, pH 8.0, 1 mM EDTA, 2.5% SDS, 5% B-mercaptoethanol), and subjected to polyacrylamide gel electrophoresis under denaturing and reducing conditions. Protein was transferred to a PVDF membrane and immunostained with a rabbit polyclonal Ab raised against a 14–amino acid peptide representing the carboxy terminus of MPO (NTLPKLNLTSWKET). Peripheral blood smears and bone marrow samples were fixed with formaldehyde and stained using the Kaplow procedure (57) with benzidine dihydrochloride and 2 μM H_2O_2.

Oxidant generation by phagocytes. Peritoneal exudate cells were elicited by injecting mice intraperitoneally with 1 ml of 4% thioglycollate broth. After 4 or 12 hours, cells were harvested by peritoneal lavage using ice-cold PBS. Cells were pelleted by centrifugation and resuspended at 1 or 2×10^6 cells/ml in PBS supplemented with 0.9 mM $CaCl_2$, 0.5 mM $MgCl_2$, 7.5 μM glucose, and 75 μM ferricytochrome c. Cells were stimulated at 37°C with 200 nM phorbol myristate acetate and maintained in suspension by intermittent agitation. Superoxide production was measured as the superoxide dismutase-inhibitable (60 μg/ml) reduction of cytochrome c (monitored at A_{550}) (58). Analysis was performed on C57BL/6J ($n > 30$/genotype) and LDL receptor–deficient (LDLR-deficient) ($n = 6$/genotype) mice. HOCl generation by activated cells was measured in PBS supplemented with 10 mM taurine. The resulting taurine chloramine was quantified by the oxidation of 5-thio-2-nitrobenzoic acid (59).

Protein oxidation products. Phagocytes were recruited into the peritoneal cavity by intraperitoneal injection with 1 ml of 4% thioglycollate broth. Twenty hours after recruitment, phagocytes were activated in situ by zymosan injection (250 mg/kg). Forty-four hours after thioglycollate injection, mice were lavaged with HBSS, and peritoneal exudate cells were pelleted by centrifugation. Cells were resuspended in PBS supplemented with 10 mM 3-aminotriazole (3-AT), 10 mM butylated hydroxytoluene (BHT), and 100 μM diethylenetriamine pentaacetic acid (DTPA), snap-frozen in liquid nitrogen, and stored at –80°C until analysis. Aortic tissues were collected from animals fed an atherogenic diet for 14 weeks. At sacrifice, animals were perfused with ice-cold PBS containing 3-AT, BHT, and DTPA, aortae were carefully dissected to remove adventitial fat, and samples were frozen in the same buffer at –80°C until analysis was performed. Cell pellets and mouse aortic tissue samples were thawed, homogenized, resuspended in water supplemented with 10 mM 3-AT and 100 μM DTPA, and delipidated three times (60). After the addition of 30 pmol of 3-[$^{13}C_6$]chlorotyrosine and 50 nmol

[$^{13}C_6$]tyrosine, delipidated proteins were dried under N_2, resuspended in 0.5 ml of HBr (48%) containing 1% phenol, and heated at 110°C for 24 hours under argon atmosphere. After hydrolysis, 0.5 ml of 0.1% trifluoroacetic acid (TFA) was added, and the solution was applied to a solid-phase C18 extraction column (3 ml Supelclean LC-18 SPE; Supelco, Bellefonte, Pennsylvania, USA) equilibrated with 0.1% TFA. The column was washed with 2 ml of 0.1% TFA, eluted with 2 ml of 50% methanol in 0.1% TFA, and the recovered amino acids were dried under vacuum. *N*-Propyl ester, heptafluorobutyryl derivatives of amino acids, were prepared as described (60).

Derivatized amino acids were analyzed on a Varian 3400 gas chromatograph interfaced with a Finnigan SSQ 7000 mass spectrometer. Amino acids were quantified by isotope dilution using selected ion monitoring in the negative-ion electron-capture mode, with methane as reagent gas (60). The ions used for detecting analyte and internal standard were: tyrosine, *m/z* 417 and 423; 3-chlorotyrosine, *m/z* 629 and 635. Chromatographic separations were performed with a 12-m DB-1 column (0.2 mm i.d., 0.33 μm film thickness; P.J. Cobert and Associates, St. Louis, Missouri, USA) employing a linear temperature gradient (150°C for 3 minutes, then increasing to 270°C at 20°C/min.) with helium as the carrier gas. The injector, transfer line, and source temperatures were 250°C, 250°C, and 200°C, respectively.

Candidal killing in vitro and in vivo. Peritoneal exudate cells were elicited by injecting mice intraperitoneally with 2.5 ml of 3% thioglycollate broth. After 4 hours, cells were harvested by peritoneal lavage using ice-cold HBSS supplemented with 1 U/ml heparin. Cells were collected by centrifugation and resuspended in HBSS supplemented with 1 mM $MgCl_2$, 5 mM $CaCl_2$, and 10 mM HEPES buffer (pH 7.4). *Candida albicans* strain 820 (61) was cultured overnight, washed by centrifugation in ice-cold water, and then opsonized at 37°C with human serum. Approximately 250 μl of 5×10^5 neutrophils were mixed with equal volumes of FCS, HBSS, and 5×10^5 opsonized *Candida*, and the mixture was incubated with constant rotation for 2 hours at 37°C. After addition of BSA (1% wt/vol), cells were pelleted on a slide by centrifugation, fixed with methanol, and stained with Giemsa. Neutrophil-ingested *Candida* were scored visually as germinated, ungerminated, or dead, based on staining characteristics (62). Briefly, germinated and ungerminated *Candida* stained blue, while dead *Candida* appeared white. Slides were assessed by two observers blinded to the source of the neutrophils.

C. albicans strain 820 was cultured on Sabouraud dextrose agar. Single colonies were isolated, grown overnight, and subcultured for 18 hours. Cells were collected by centrifugation, washed in ice-cold water, and resuspended in sterile normal saline. Inocula were prepared and injected into the peritoneal cavity of mice. Animal health was monitored daily. For histology, kidneys were excised, fixed in 10% neutral buffered forma-

lin, embedded in paraffin, sectioned, and stained with Gomori's methenamine silver (Sigma Chemical Co., St. Louis, Missouri, USA). For colony counts, kidneys were harvested, weighed, and homogenized in HBSS. Samples were diluted, plated on Sabouraud dextrose agar plates, and incubated at 37°C overnight.

Bone marrow transplantation. The *MPO* mutant allele was backcrossed onto the C57BL/6J background and resultant male heterozygous (*MPO+/–*) animals were screened for residual 129/SvJ loci at approximately 20-cM intervals spanning the mouse genome as described (63). This "marker-assisted selection protocol" strategy was used to select for male animals with the highest contribution of C57BL/6J loci, which are therefore more inbred (63). The donor mice for bone marrow harvesting were approximately 91% C57BL/6J, and the major histocompatibility haplotype (H-2^b) is the same between C57BL/6J and 129/SvJ. Ten-week-old LDLR-deficient mice were irradiated with 11 Gy of total body radiation. Bone marrow was flushed from the femurs and tibias of donor mice and 10^7 bone marrow cells were injected into the tail vein of recipient LDLR-deficient mice to rescue the lethally irradiated animals (64). Animals were maintained in autoclaved cages with microisolator lids and autoclaved water in a specific pathogen-free facility screened quarterly for pneumonia virus of mice, mouse hepatitis virus, minute virus of mice, mouse Parvovirus, *Mycoplasma pulmonis*, Theiler's mouse encephalomyelitis virus, Sendai virus, lymphocytic choriomeningitis virus, epizootic diarrhea of infant mice, ectromelia virus, Reovirus, *Aspiculuris tetraptera*, and *Syphacia obvelata*.

Atherosclerosis assessment. Mice were fed a chow diet immediately following transplantation. Starting 5 weeks after transplantation, animals were fed a high-fat diet (16% fat, 1.25% cholesterol, 0% cholate; Harlan Teklad Laboratory, Winfield, Iowa, USA) for 14 weeks. At 5 and 19 weeks after transplantation, animals were fasted for 16 hours and bled via the retro-orbital sinus under Aerrane anesthesia. Determination of plasma triglyceride and cholesterol levels and analyses of plasma lipoproteins by high-resolution size-exclusion fast protein liquid chromatography (FPLC) were performed as previously described (65). At sacrifice, white cell counts were performed on white blood cell samples using a Hemavet Hematology analyzer (CDC Technologies Inc., Oxford, Connecticut, USA) that enumerates cells based on size and internal complexity. Bone marrow cells were flushed from mouse femurs, fixed onto microscope slides, and staining was performed using benzidine dihydrochloride as substrate for peroxidase reaction as described above. MPO deficiency was confirmed by positive peroxidase stain in eosinophils and negative peroxidase stain in neutrophils and monocytes in the same microscope field.

Animals were sacrificed and perfused through the left ventricle of the heart with PBS for 5 minutes followed by 4% paraformaldehyde/5% sucrose for 15 minutes (66). The adventitia was dissected from the aorta down to the iliac bifurcation. The heart and attached aorta were removed from the body and severed at the ascending aorta. The heart and proximal aorta were embedded in OCT compound, sectioned, stained with oil red O for neutral lipids, and lesions were then quantified using standard procedures (67). Aortic lesion area was quantified using serial cross-sections obtained every 50 μm, beginning at the termination of the aortic valve and spanning 400 μm of ascending aorta. For en face analysis of atherosclerotic lesion area, aortae were cut longitudinally and stained with Sudan IV (66). Tissue was pinned and photographed, and total surface area and lesion area in an approximately 10-mm-long section of ascending and thoracic aorta were quantified using a computerized image analysis program (Image Pro Plus; Media Cybernetics, Silver Spring, Maryland, USA). A similar total surface area was measured for each of the animals.

In addition to bone marrow transplantation studies, the *MPO* mutant allele was also backcrossed onto the C57BL/6J (75%, 91% C57BL/6J) and LDLR-deficient (96% C57BL/6J) backgrounds and heterozygous mating used to generate MPO-deficient and wild-type littermates. At 2 months of age, animals were placed on a high-fat, high-cholesterol diet with (C57BL/6J) or without (LDLR-deficient) cholate for 16 or 14 weeks, respectively. Hearts were isolated for lesion analysis. Proximal aorta containing grossly visible lipid accumulation and distal aorta lacking visible lipid accumulation were collected from LDLR-deficient animals for 3-chlorotyrosine determination. Aortae were also collected 2 weeks and 14 weeks after high-fat feeding, and Western blot analysis was performed as described above.

Immunohistochemistry. Analyses were performed on lesions from the aortic root as described previously (67). Sections were fixed in acetone and incubated with a rat polyclonal Ab to mouse monocyte/macrophage MOMA-2 (Accurate Chemical & Scientific Corp., Westbury, New York, USA), rabbit polyclonal Ab to smooth muscle cell tropomyosin (Sigma Chemical Co.), or rabbit polyclonal Ab to mouse MPO peptide (described above), followed by anti-rat or anti-rabbit secondary Ab's. Detection was performed with peroxidase chromogen kit (Vector Laboratories, Burlingame, California, USA).

Statistical analyses. Values represent the mean plus or minus SE. Differences between groups were evaluated by Student's *t* test.

Results

Targeted disruption of the mouse MPO gene prevents MPO expression. The crystal structure of MPO reveals two identical subunits; in each half, proteolytic processing of a precursor polypeptide yields a heavy chain containing the catalytic heme group and a light-chain (68). The gene-targeting strategy used was to insert a neomycin resistance gene and premature stop codon at the end of the light chain (Figure 1a). This insertion was expected to inactivate MPO because the light chain is proximal to the heavy chain and because the targeted portion is involved in heme binding (68). Targeting

was performed, and a total of 420 G418/ganciclovir double-resistant embryonic stem cell colonies were screened. Three candidate clones were identified, and one cell line produced chimeras that transmitted the MPO mutation (Figure 1b). MPO was not detected by Northern blot (Figure 1c) or Western blot analysis (Figure 2e) of bone marrow from animals homozygous for the inserted mutation. The mice grew normally, were apparently healthy, and exhibited Mendelian transmission of the mutant allele. Their total white blood cell counts and differentials were similar to wild-type animals (wild-type: $17 \pm 4 \times 10^3$ cells/μl, $18 \pm 9\%$ neutrophils, $5 \pm 1\%$ monocytes, $3 \pm 1\%$ eosinophils, $74 \pm 8\%$ lymphocytes; MPO-deficient: $16 \pm 4 \times 10^3$ cells/μl, $14 \pm 3\%$ neutrophils, $5 \pm 2\%$ monocytes, $3 \pm 1\%$ eosinophils, $78 \pm 3\%$ lymphocytes; $n = 6$).

MPO-deficient neutrophils do not produce hypochlorous acid. MPO is characterized by peroxidase and chlorination activities, and both functions were assayed in mutant and control animals. Peripheral blood smears and bone marrow isolates were harvested, fixed on slides, and stained for in situ peroxidase activity. Neutrophils and monocytes from both peripheral blood and bone marrow of mutant animals failed to exhibit endogenous peroxidase activity (Figure 2, b and d). In contrast, eosinophils, which possess the functionally distinct gene product eosinophil peroxidase, demonstrated peroxidase staining (Figure 2d). The ability of leukocytes to generate hypochlorous acid was determined using thioglycollate-elicited cells isolated from the peritoneum of wild-type and mutant animals. Neutrophils predominated in the elicited cell populations in both MPO-deficient and wild-type mice (wild-type: $67 \pm 4\%$ neutrophils, $30 \pm 4\%$ mononuclear cells, $0.5 \pm 0.3\%$ eosinophils; MPO-deficient: $72 \pm 4\%$ neutrophils, $25 \pm 3\%$ mononuclear cells, $0.8 \pm 0.2\%$ eosinophils; $n = 6$). Cells were activated with phorbol myristate acetate, and HOCl production was measured by monitoring formation of *N*-mono-chlorotaurine. After a 1.5-hour incubation at 37°C, wild-type cells (2×10^6/ml) generated 7.0 ± 2.7 μM HOCl (Figure 3a). HOCl production by MPO-deficient cells, in contrast, was undetectable.
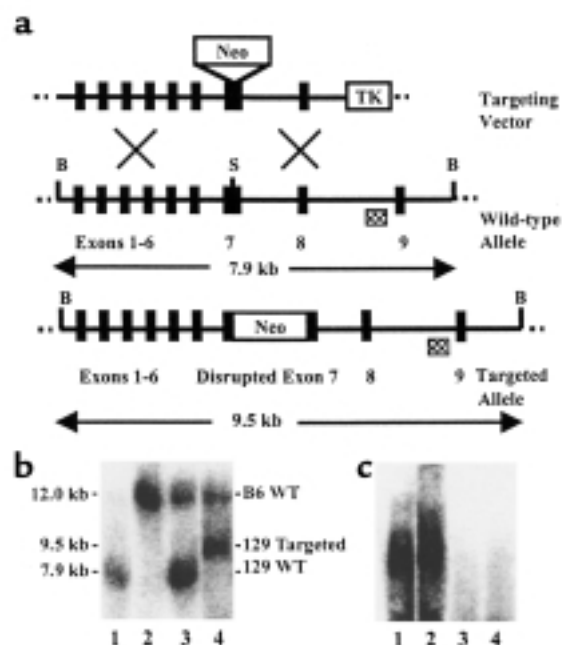
In parallel studies, the rate of superoxide production by thioglycollate-elicited peritoneal exudate cells was measured. Isolated cells were stimulated with phorbol myristate acetate and the reduction of ferricytochrome c monitored in the presence or absence of superoxide dismutase. The kinetics and cumulative level of superoxide production by wild-type and mutant cells were similar for both genotypes on the C57BL/6J (data not shown) and LDLR-deficient backgrounds (Figure 3b).

Activated phagocytes from MPO-deficient mice fail to chlorinate proteins in vivo. To determine whether HOCl produced by MPO chlorinates proteins in vivo, isotope dilution gas chromatography/mass spectrometry (GC/MS) was used to quantify total protein-bound 3-chlorotyrosine of resident peritoneal cells, thioglycollate-elicited peritoneal exudate cells, and thioglycollate-elicited peritoneal exudate cells activated in situ with zymosan. The latter is a component of the yeast cell wall that is rapidly phagocytosed by neutrophils in vitro (3). Neutrophils predominated in this population of cells, and the relative amounts of neutrophils and monocyte/macrophages did not differ significantly between the two types of mice.

Resident and thioglycollate-elicited cells from wild-type and MPO-deficient animals exhibited low levels of 3-chlorotyrosine (Figure 4). However, when zymosan

Figure 1

Targeted disruption of the mouse *MPO* gene. (**a**) The targeting vector, wild-type *MPO* locus (including exons 1–9), and targeted *MPO* gene are shown. Exon 7 was disrupted by insertion of positive-selection marker PGK-Neo (Neo) at a *Bss*HII (S) site. HSV-thymidine kinase (TK) served for negative selection. *Bgl*II (B) digestion sites, lengths of diagnostic *Bgl*II fragments, and external probe (checkered box) used for Southern blot analysis are indicated. (**b**) DNA isolated from progeny of chimeric founder male mated with C57BL/6J female was subjected to *Bgl*II digestion and Southern blot analysis. Lanes 1 and 2 contained the wild-type controls 129/SvJ DNA (lane 1) and C57BL/6J DNA (lane 2). Note the difference in band size between the two strains, indicative of a restriction fragment length variant. Strain 129/SvJ has *Bgl*II restriction enzyme sites at nucleotides 189 and 8075, yielding a 7.9-kb product, whereas C57BL/6J is lacking one of these sites, and the fragment generated represents digestion at a more distal *Bgl*II site. Restriction variants, such as this one, are due to naturally occurring nucleic acid sequence differences between inbred strains. Lanes 3 and 4 are from progeny. The larger band in both lanes is inherited from the C57BL/6J mother, and the lower band, inherited from the chimeric father, is either wild-type (lane 3) or targeted (lane 4). (**c**) RNA samples isolated from bone marrow from wild-type (lanes 1 and 2) and mutant (lanes 3 and 4) mice were subjected to Northern blot analysis with a human cDNA probe.

was injected into the peritoneum of wild-type animals exposed to thioglycollate for 20 hours, 3-chlorotyrosine levels increased markedly in the recruited cells (Figure 4). Protein chlorination reached a plateau 2 hours after zymosan stimulation and remained elevated for 48 hours (data not shown). In marked contrast, 3-chlorotyrosine levels were not elevated in cells from mice that lacked MPO despite similar treatment (Figure 4).

MPO deficiency impairs the ability to kill C. albicans. To determine if neutrophils from MPO-deficient mice exhibit a defect in fungal killing similar to that observed in MPO-deficient humans, peritoneal exudate cells were isolated by lavage from thioglycollate-stimulated animals. Cells were then incubated for 2 hours at 37°C with serum-opsonized *C. albicans* (1:1; neutrophil/*Candida*) and microscopically assessed for the extent to which they had ingested and killed the fun-

gus. Lack of cytoplasmic staining with Giemsa indicated *Candida* killing; germ tube formation inside neutrophils indicated that *Candida* had survived and germinated. Wild-type neutrophils killed 55% of the ingested *Candida*. In contrast, only 18% of *Candida* ingested by MPO-deficient neutrophils were dead ($P = 0.001$). Moreover, *Candida* was able to replicate inside MPO-deficient neutrophils: 30% of ingested *Candida* germinated in MPO-deficient neutrophils, whereas only 4% germinated inside phagocytic vesicles of neutrophils from the wild-type mice ($P = 0.005$).

To test the in vivo relevance of this killing mechanism, we challenged wild-type and MPO-deficient animals with *C. albicans*. Inoculum of 10^8 *Candida* per animal resulted in 40% mortality in MPO-deficient mice by 20 days after intraperitoneal injection (Figure 5). In contrast, all wild-type animals were alive at day 65. At 6×10^8 *Candida* per animal, all of the MPO-deficient mice were dead by day 7. Again, no deaths occurred in their normal littermates by day 65. Fungal infiltration of the kidney is a prominent pathological component of disseminated *Candida* infection in animals (reviewed in ref. 69). Kidneys of infected animals were examined for *Candida* by using immunohistochemistry and by culturing tissue samples. Both tests were positive in MPO-deficient mice, but negative in wild-type animals (data not shown).

MPO-deficient mice develop larger atherosclerotic lesions. To examine the possible involvement of MPO in atherogenesis, we used bone marrow transplantation to create combined MPO-deficient, LDLR-deficient mice. Bone marrow from MPO-deficient and wild-type animals was harvested and injected into irradiated LDLR-deficient animals. Ablation of LDLR-deficient bone marrow progenitors and reconstitution with MPO-deficient or wild-type donor bone marrow was confirmed in transplanted animals by staining peripheral blood cells and bone marrow for peroxidase activity (data not shown). After a 5-week period to allow engraftment, mice were fed a high-fat, high-cholesterol diet for 14 weeks. The white cell counts were normal and similar between the two groups at sacrifice (MPO wild-type/LDLR-deficient: $16.7 \pm 1.9 \times 10^3$ cells/μl, $n = 7$; MPO-deficient/LDLR-deficient: $17.1 \pm 2.5 \times 10^3$ cells/μl, $n = 7$). Plasma lipoprotein analysis performed 5 weeks after transplantation revealed no differences between groups (Table 1). The two groups also had similar plasma lipoprotein levels after 14 weeks of high-fat feeding (Table 1), and lipoprotein profiles were similar as determined by high-resolution size-exclusion FPLC (Figure 6). Animals gained weight at the same rate and were apparently healthy at sacrifice.

The extent of atherosclerosis was determined by measuring cross-sectional area of lesions in the proximal aorta and through en face analysis of the aortic surface. Cross-sectional analysis indicated that lesions in MPO-deficient mice were about 50% larger than controls (Figure 7). MPO wild-type/LDLR-deficient mice exhibited an average lesion area of $24.5 \pm 1.6 \times 10^4$
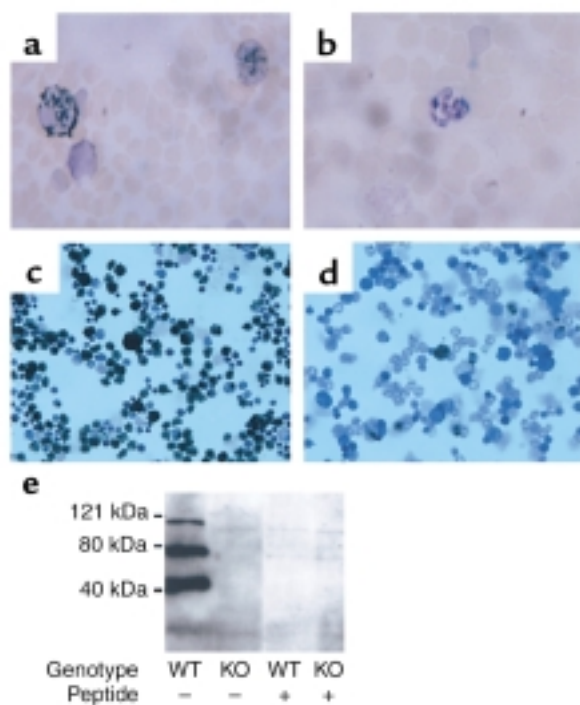

Figure 2
Functional ablation of the *MPO* gene. Peroxidase stains were performed on *MPO+/+* (**a**) and *MPO–/–* (**b**) peripheral blood samples and *MPO+/+* (**c**) and *MPO–/–* (**d**) bone marrow samples. Cell types were determined based on nuclear staining and size. Shown are peroxidase-positive eosinophil(s) (**a**, **c**, **d**), neutrophil(s) (**a**, **c**), and monocytes (**c**), and peroxidase-negative neutrophil(s) (**b**, **d**) and monocytes (**d**). Bone marrow cells from *MPO+/+* and *MPO–/–* mice were subjected to SDS-PAGE. Western blot analysis (**e**) was performed with a rabbit polyclonal Ab against the carboxy-terminal 14 amino acids of MPO. The peptide immunogen was used in indicated lanes to block immunoreactivity. MPO is synthesized as a preproenzyme and undergoes processing. The three major bands in the wild-type mice likely represent prepro-MPO, processed (but unclipped) heavy and light chains of MPO, and the heavy chain of MPO. Microsatellites of molecular-weight-size markers are indicated.
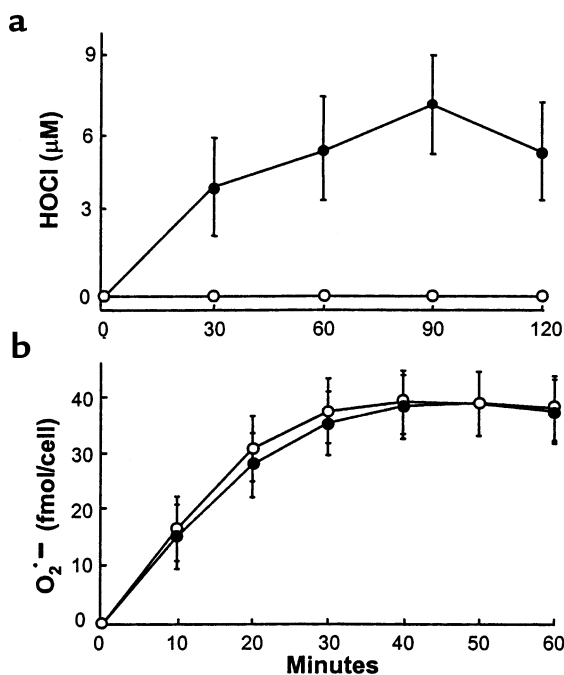
Figure 3

Superoxide and hypochlorous acid production by peritoneal phagocytes in vitro. (**a**) Peritoneal exudate cells were isolated from thioglycollate-treated wild-type (filled circle) or MPO-deficient (open circle) animals ($n = 4$/genotype) and stimulated with phorbol ester, and HOCl production was measured as taurine chloramine formation. (**b**) Peritoneal exudate cells were isolated from thioglycollate-treated wild-type (filled circle) or MPO-deficient (open circle) LDLR-deficient animals ($n = 6$/genotype) and stimulated with phorbol ester, and superoxide ($O_2^{\cdot-}$) production was quantitated as the reduction of cytochrome c.

μm^2/section, whereas MPO-deficient/LDLR-deficient mice exhibited an average lesion area of $37.3 \pm 2.8 \times 10^4$ μm^2/section ($n = 21$ per group, $P = 0.0003$). En face analysis to examine the extent of lesion formation throughout the aorta was performed on a subset of the animals. Lesional surface area in MPO wild-type/LDLR-deficient mice was $2.3 \pm 0.4\%$ of aortic surface area ($n = 9$) and in MPO-deficient/LDLR-deficient animals was $3.5 \pm 0.5\%$ of aortic surface area ($n = 11$). Although the results did not reach statistical significance ($P = 0.07$), they were consistent with the cross-sectional analysis with about a 50% increase in lesion area in the MPO-deficient mice. Lesion analyses were also performed as the mice were being backcrossed onto the C57BL/6J background. At no point measured (75%, 91% C57BL/6J) was there a detrimental effect observed for MPO on fatty streak lesion formation. Mice were also backcrossed onto the LDLR-deficient background, fed a high-fat diet, and results (wild-type: $46.1 \pm 2.1 \times 10^4$ μm^2/section, $n = 13$, vs. MPO-deficient: $54.4 \pm 2.0 \times 10^4$ μm^2/section, $n = 12$; $P = .0099$) consistent with the bone marrow transplantation data were observed.

Complex lesions with fibrous caps were visible in both MPO wild-type and MPO-deficient mice (Figure 8, a and b). Calcification was observed in both genotypes. To determine if MPO deficiency affected the cellular composition of the lesions, staining with Ab's specific for monocytes (Figure 8, c and d) and smooth muscle cells (Figure 8, e and f) was performed. The MPO-deficient animals appeared to have increased monocyte number, consistent with larger lesion area.

Mouse atherosclerotic lesions contain low levels of 3-chlorotyrosine. We next examined the lesions for the presence of MPO and evidence of its catalytic activity. Before our laboratory initiated the generation of MPO-deficient mice, we examined and detected MPO immunostaining in the shoulder region of advanced atherosclerotic lesions in mice (Figure 8g), similar to that which is reported in human lesions (7). However, immunostaining in the knockout mice revealed a similar staining pattern (Figure 8h). The Ab's used did not show any reactivity in Western blot analysis of bone marrow or peripheral blood lysates derived from MPO-deficient mice, but do so in those from the wild-type mice (Figure 2e). Several additional Ab's against either human or

mouse MPO were evaluated. All but one showed cross-reactivity in aortic tissue from MPO-deficient mice. Subsequent RT-PCR and Western blot analyses of early and advanced atherosclerotic lesion tissue from both wild-type and MPO-deficient mice failed to reproducibly demonstrate the presence of MPO in murine atherosclerotic tissue. To assay for evidence of MPO activity in aortic tissue, chlorotyrosine content was measured in aortic arch containing and abdominal aorta lacking visible lipid accumulation. In contrast to results observed with the acute inflammation model (Figure 4), chlorotyrosine levels in aortic lesion tissue were barely detectable and did not differ between MPO-deficient and wild-type animals (Table 2). The trace levels of chlorotyrosine observed in aortic lesions were not significantly higher than those seen in normal aortic tissue from the same animal (Table 2).

Table 1

Plasma lipids in MPO-deficient/LDLR-deficient and MPO wild-type/LDLR-deficient animals

	Total cholesterol (mg/dl)	HDL cholesterol (mg/dl)	Triglycerides (mg/dl)
Chow diet			
$MPO^{+/+}$	327.7 ± 6.8	105.2 ± 2.9	220.5 ± 22.0
$MPO^{-/-}$	333.0 ± 6.1	105.4 ± 2.1	228.3 ± 30.6
Atherogenic diet			
$MPO^{+/+}$	930.8 ± 51.3	97.9 ± 3.7	155.2 ± 11.1
$MPO^{-/-}$	837.0 ± 33.8	94.1 ± 3.1	169.1 ± 11.2

LDLR-deficient animals were bone marrow transplanted with either MPO-deficient or MPO wild-type bone marrow and fed a chow diet for 5 weeks. Animals ($n = 21$ per group) were fasted for 16 hours and bled, and plasma total cholesterol, HDL cholesterol, and triglycerides were determined as described in Methods. Mice were fed a diet consisting of 1.25% cholesterol for 14 weeks, at which time they were bled and plasma total cholesterol, HDL cholesterol, and triglycerides were determined.
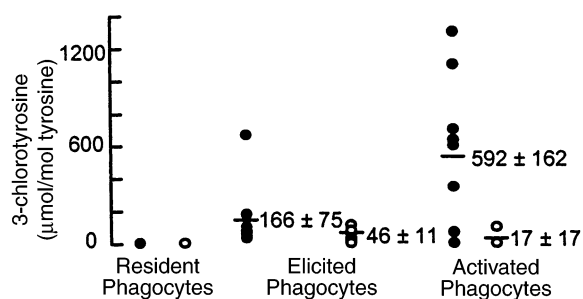
Figure 4
Isotope-dilution GC/MS analysis of 3-chlorotyrosine in phagocytes isolated from *MPO+/+* and *MPO−/−* mice. Resident peritoneal cells (resident phagocytes; $n = 3$), thioglycollate-elicited peritoneal exudate cells (quiescent phagocytes; *MPO+/+*, $n = 8$, and *MPO−/−*, $n = 10$), and thioglycollate-elicited, zymosan-stimulated peritoneal exudate cells (activated phagocytes; *MPO+/+*, $n = 8$, and *MPO−/−*, $n = 6$) were isolated by lavage from wild-type (filled circle) and MPO-deficient (open circle) animals. After acid hydrolysis and derivatization, 3-chlorotyrosine levels of cellular proteins were determined by negative-ion electron capture GC/MS with selected ion monitoring. Results are normalized to tyrosine, the precursor amino acid.

Discussion

We generated MPO-deficient mice to explore the possible role(s) of MPO in inflammation. MPO was not detected in bone marrow cells isolated from these animals, and peritoneal phagocytes failed to generate HOCl in vitro, indicating that the phagocytes of the mutant mice lack functional MPO. Like humans that are MPO deficient, the mice were apparently healthy, and their neutrophils exhibited impaired candidacidal activity. Infection with *C. albicans* resulted in 100% mortality in MPO-deficient mice and no mortality in wild-type littermates. To examine the possible role of MPO in inflammatory disease, we challenged the mice with hyperlipidemia, which resulted in advanced atherosclerosis. We also examined the role of MPO in protein modification that may serve as a marker of MPO involvement in tissue damage during inflammation. The results

Table 2
3-Chlorotyrosine levels in mouse aortae

Normal tissue	(µmol/mol)
MPO+/+	33 ± 21
MPO−/−	25 ± 25
Lesioned tissue	
MPO+/+	53 ± 23
MPO−/−	68 ± 24

MPO-deficient or wild-type animals on the LDLR-deficient background were fed an atherogenic diet for 14 weeks. Animals were perfused with antioxidant buffer and grossly normal and lesioned aortae were isolated for 3-chlorotyrosine quantitation. Results are normalized to tyrosine, the precursor amino acid.

demonstrate the importance of MPO in protein chlorination in vivo and suggest that MPO can exert a protective effect in at least one inflammatory disease, atherosclerosis. They also question the presence of MPO in mouse atherosclerotic lesions and indicate that MPO-mediated oxidation of biological targets within atherosclerotic tissues (as assessed by chlorotyrosine determinations) is significantly less in the mouse model than in the human disease.
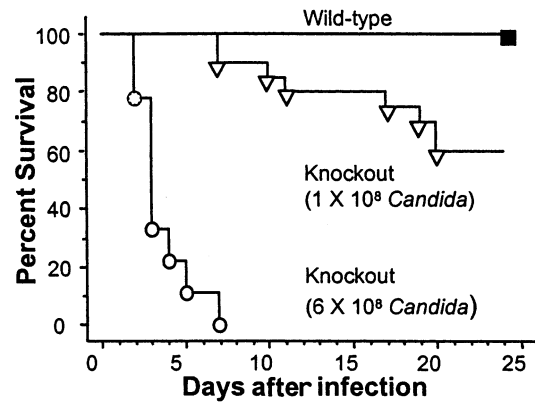
We tested the role of MPO in atherosclerosis using LDLR-deficient mice. These mice represent a mouse model of familial hypercholesterolemia, and when fed a high-fat, high-cholesterol diet they, like humans, develop large atherosclerotic lesions with foam cells and fibrous caps (70). Because MPO is expressed in bone marrow–derived cells, we were able to produce combined MPO-deficient/LDLR-deficient mice using bone marrow transplantation. Bone marrow transplants have been used previously in a variety of atherosclerosis studies in mice (61, 71, 72). We used as donors MPO-deficient mice in which the targeted MPO allele was placed on the background of strain C57BL/6J by a "marker-assisted selection protocol" (63). Potential problems resulting from genetic heterogeneity were further minimized by the fact that the host LDLR-deficient mice were on a C57BL/6J background.

Our results revealed a clear, approximately 50% increase in atherosclerotic lesions in the MPO-deficient mice as compared with the wild-type mice. The lesions were examined in large groups of mice (21 per group) due to the nongenetic variance in lesion development known to occur (73). Lesions were determined using both cross-sectional area in the proximal aorta as well as by en face examination of the entire aortic tree. Both methods yielded similar results although the cross-sectional method gave more significant findings due to reduced nongenetic variance and a larger sample size. We observed no evidence of rejection or graft-versus-host disease, and there were no differences in white cell counts or in circulating lipoprotein levels between the groups. Animals were maintained in a specific pathogen-free facility to limit chances of infection. Experimental artifacts are unlikely since the bone marrow transplantations were performed in two independent experiments and no differences were obtained between deficient mice and between wild-type mice transplanted on different days. Moreover, studies with MPO-deficient mice backcrossed onto the LDLR-deficient background and fed a high-fat diet for 14 weeks yielded consistent, statistically significant results.

Our results indicating a protective effect for MPO in lesion development are surprising because oxidation has been considered a promoting influence in atherosclerosis and other chronic diseases (45–47). This is based largely on the reasoning that oxidants react with and are directly damaging to the structural makeup of cells, surrounding matrices, and key functional pathways. The oxidation of biological targets could, how-

Survival of *MPO*^{+/+} and *MPO*^{−/−} mice after intraperitoneal challenge with *Candida*. Each mouse was injected with 10^8 CFU of *C. albicans* (*MPO*^{+/+}, *n* = 19; *MPO*^{−/−}, *n* = 19) or 6×10^8 CFU of *C. albicans* (*MPO*^{+/+}, *n* = 9; *MPO*^{−/−}, *n* = 9). Survival was monitored for 65 days, and no mortality occurred after 20 days. Results are from two independent experiments.

ever, conceivably have many positive effects. There are experimental data linking MPO to the oxidative inactivation of proinflammatory molecules, including chemotactic proteins (74), activation of proteases that could affect leukocyte infiltration (75), alterations of lymphocyte functions (76), and effects on the production of inflammatory mediators (77, 44), cholesterol efflux (78), and lipoprotein turnover (79). MPO could also influence the proliferation and apoptosis of macrophages and smooth muscle cells through effects on production of oxidized lipids (44), or regulation of NO (80), or NO-derived oxidants (42–44). Alternatively, a protective action of MPO with regard to atherosclerosis development may be due to impaired capacity to kill some unknown pathogen(s) or to clear noxious stimuli that promote atherogenesis, such as oxidized LDL (43, 51, 53). MPO could arguably be acting at any of the three stages of atherosclerosis — initiation, progression, or complication — and might have both pro- and antiatherogenic effects.

Mouse-human species differences may be relevant in interpreting the role of phagocyte-inflicted injury using this model. MPO levels (per neutrophil) are fivefold to tenfold higher in the human than in the mouse (20, 81), and MPO regulation, including active promoters (82) and inducers, may differ significantly. In contrast to human atheroma that readily stain for MPO and show clear evidence of chlorotyrosine (474 μmol/mol; ref. 22), the chloroty-

rosine levels (53 μmol/mol) observed in the mouse are barely above the limit of detection. While it is not known if they are bona fide levels or background noise generated as artifact during sample handling, the trace levels observed argue that MPO is not catalytically active in the artery wall in the mouse model. Polyclonal Ab's against MPO showed MPO immunostaining in lesions from wild-type and deficient mice. It is highly unlikely that this staining represents bona fide MPO. Functional ablation of MPO in knockout animals has been confirmed by demonstrating loss of MPO RNA in marrow, loss of anti-MPO heavy-chain immunostaining in bone marrow cells and peripheral leukocytes, loss of in situ peroxidase-activity staining in these cell populations, and loss of HOCl-generating activity in the MPO-deficient leukocytes both in vitro (isolated leukocytes) and in vivo (peritonitis model). Moreover, MPO was not detectable by Western blotting in atherosclerotic tissue from LDLR-deficient and apolipoprotein E–deficient mice. The reason for the apparent cross-reactivity in atheroma from bone marrow–transplanted animals is unclear. It may be that there exists a MPO heavy-chain homologue.

Oxidative and antioxidant pathways may also differ and/or be induced differently in the mouse versus the human. For example, our candidacidal activity assay showed that mouse neutrophils exhibited impaired, but not abolished, ability to kill *C. albicans*. This resid-

Figure 6

FPLC fractionation and cholesterol determination of plasma from MPO wild-type/LDLR-deficient and MPO-deficient/LDLR-deficient animals. Mice were fed an atherogenic diet for 14 weeks. After a 16-hour fast, they were bled, equal amounts of plasma from eight animals in each group were pooled, and FPLC was performed. Total cholesterol was determined in fractions as described (65).
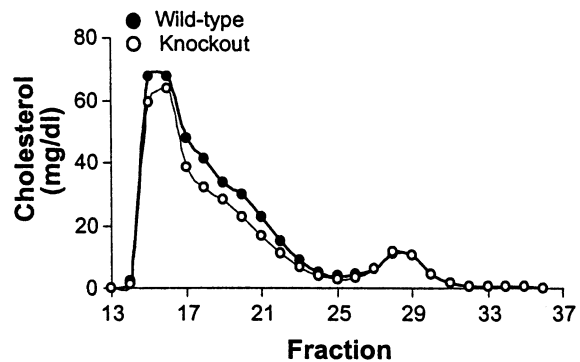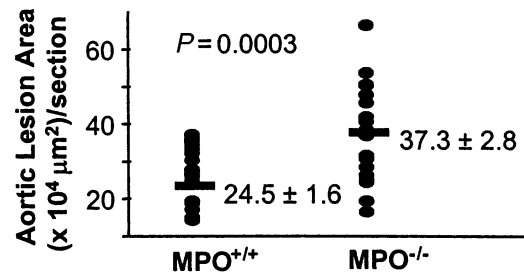
Figure 7

Effect of MPO deficiency on atherosclerosis development in mice. LDLR-deficient mice that were also MPO wild-type or deficient were fed an atherogenic diet for 14 weeks, and atherosclerosis was assessed. The total lesion areas in sections from the proximal aorta of LDLR-deficient mice containing the wild-type or targeted MPO allele were determined using oil red O staining. Values for individual animals ($n = 21$ per group) are shown.
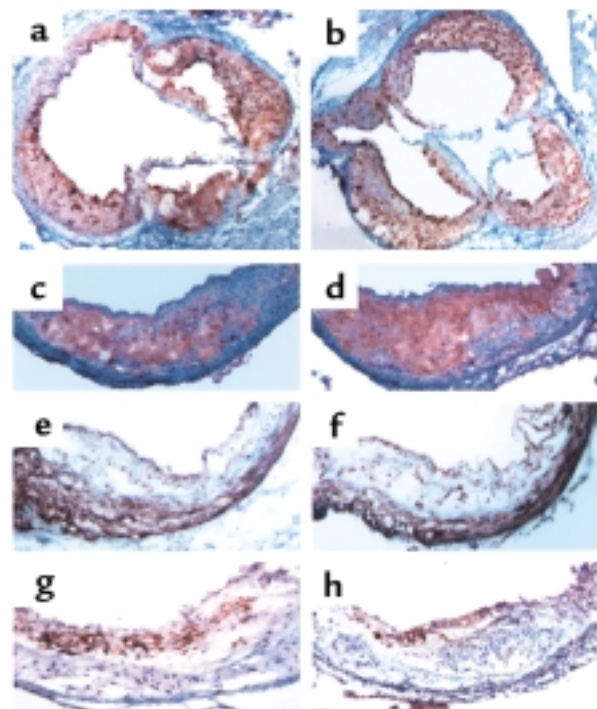
ual candidacidal activity contrasts with the complete absence exhibited by human MPO-deficient neutrophils (16). This could reflect differences in host defense mechanisms of an oxidative nature, such as the higher expression of nitric oxide that is seen in rodent neutrophils (83) or other compensatory host defense mechanisms. MPO can impact on production of reactive nitrogen species (40–44) and levels of nitric oxide (80), and nitric oxide can impact upon MPO activity (84), adding additional levels of complexity. Antioxidant defense system differences in the mouse versus the human may also contribute to differences observed in MPO activity in atherosclerotic tissue. Ascorbate, a potent inhibitor of MPO-catalyzed chlorination, is an essential vitamin in humans, but not in mice (85). Human MPO-deficient neutrophils have been reported to have a prolonged respiratory burst (86). We failed to observe a significant difference in either duration or initial rate using our animal model. The NADPH-oxidase system is the primary source of leukocyte-reduced oxygen species for MPO-dependent reactions. Ablation of this gene has been shown

recently to have no effect on murine atherosclerosis (87). Whether there is upregulation or use of alternative superoxide generating systems (88) is not known. The results of the present studies and those with NADPH-oxidase–null mice (87) invite a reappraisal of the role of oxidation in mouse models of atherosclerosis. They also caution against the assumption that murine models can be used to study a given mechanism without demonstration of its potential relevance to the human correlate.

The limited levels of MPO and HOCl oxidation products observed in mouse atheroma might superficially suggest that the murine model is of uncertain relevance for studies of MPO in atherosclerosis, a chronic inflammatory diseases. However, the increase in lesion progression implicates a previously unsuspected function that is likely acting systemically and is not mediated simply at the local arterial level. Further studies are warranted to identify the underlying mechanism(s). The murine models of acute inflammation and infection used demonstrated robust levels of oxidant production and phenotypes analogous

Figure 8

Atherosclerosis in MPO wild-type/LDLR-deficient and MPO-deficient/LDLR-deficient animals. Cross-sections through the aortic root were stained with oil red O to detect neutral lipid in wild-type (**a**) and MPO-deficient (**b**) animals. Extensive lesions are visible. Immuno-histochemical stains for monocyte/macrophages in wild-type (**c**) and MPO-deficient (**d**) animals are shown with intense red staining. Smooth muscle cell staining in wild-type (**e**) and MPO-deficient (**f**) lesions is detected with dark brown staining and was similar between groups. Staining with Ab's against MPO in wild-type (**g**) or MPO-deficient (**h**) animals showed cross-reactivity.

to those observed in humans with MPO deficiency. The MPO-deficient animals developed should thus provide a powerful tool for exploring the role of MPO-generated oxidants in inflammation.

1. Agner, K. 1941. Verdoperoxidase: a ferment isolated from leukocytes. *Acta Physiol. Scand.* **2**:1–62.
2. Babior, B.M. 1978. Oxygen-dependent microbial killing by phagocytes. *N. Engl. J. Med.* **298**:659–666.
3. Klebanoff, S.J., and Clark, R.A. 1978. *The neutrophil: function and clinical disorders.* Elsevier/North Holland Biomedical Press. Amsterdam, The Netherlands. 1–810.
4. Weiss, S.J. 1989. Tissue destruction by neutrophils. *N. Engl. J. Med.* **320**:365–376.
5. Shultz, J., and Kaminker, K. 1962. Myeloperoxidase of the leucocyte of normal human blood. 1. Content and localization. *Arch. Biochem. Biophys.* **96**:465–467.
6. Bos, A., Wever, R., and Dirk, R. 1978. Characterization and quantification of the peroxidase in human monocytes. *Biochim. Biophys. Acta.* **525**:37–44.
7. Daugherty, A., Rateri, D.L., Dunn, J.L., and Heinecke, J.W. 1994. Myeloperoxidase, a catalyst for lipoprotein oxidation, is expressed in human atherosclerotic lesions. *J. Clin. Invest.* **94**:437–444.
8. Nagra, R.M., et al. 1997. Immunohistochemical and genetic evidence of myeloperoxidase involvement in multiple sclerosis. *J. Neuroimmun.* **78**:97–107.
9. Harrison, J.E., and Schultz, J. 1976. Studies on the chlorinating activity of myeloperoxidase. *J. Biol. Chem.* **251**:1371–1374.
10. Foote, C.S., Goyne, T.E., and Lehrer, R.I. 1981. Assessment of chlorination by human neutrophils. *Nature.* **301**:715–716.
11. Weiss, S.J., Test, S.T., Eckmann, C.M., Ross, D., and Regianai, S. 1986. Brominating oxidants generated by human eosinophils. *Science.* **234**:200–202.
12. Klebanoff, S.J. 1967. A peroxidase-mediated antimicrobial system in leukocytes. *J. Clin. Invest.* **46**:1078–1085.
13. Klebanoff, S.J. 1970. Myeloperoxidase: contribution to the microbicidal activity of intact leukocytes. *Science.* **167**:195–196.
14. Nauseef, W.M. 1988. Myeloperoxidase deficiency. *Hematol. Oncol. Clin. North Am.* **2**:135–158.
15. Petrides, P.E. 1998. Molecular genetics of peroxidase deficiency. *J. Mol. Med.* **76**:688–698.
16. Lehrer, R.I., and Cline, M.J. 1969. Leukocyte myeloperoxidase-deficiency and disseminated candidiasis: the role of myeloperoxidase in resistance to *Candida* infection. *J. Clin. Invest.* **48**:1478–1488.
17. Lehrer, R.I., Hanifin, J., and Cline, M.J. 1969. Defective bactericidal activity in myeloperoxidase-deficient human neutrophils. *Nature.* **223**:78–79.
18. Klebanoff, S.J. 1980. Oxygen metabolism and the toxic properties of phagocytes. *Ann. Intern. Med.* **93**:480–489.
19. Heinecke, J.W. 1997. Mechanisms of oxidative damage of low density lipoprotein in human atherosclerosis. *Curr. Opin. Lipid.* **8**:268–274.
20. Podrez, E.A., Abu-Soud, H., and Hazen, S.L. 2000. Myeloperoxidase-generated oxidants and atherosclerosis. *Free Radic. Biol. Med.* **28**:1717–1725.
21. Hazell, L.J., et al. 1996. Presence of hypochlorite-modified proteins in human atherosclerotic lesions. *J. Clin. Invest.* **97**:1535–1544.
22. Hazen, S.L., and Heinecke, J.W. 1997. 3-chlorotyrosine, a specific marker of myeloperoxidase-catalyzed oxidation, is markedly elevated in low density lipoprotein isolated from human atherosclerotic intima. *J. Clin. Invest.* **99**:1–7.
23. Malle, E., et al. 1997. Immunological evidence for hypochlorite-modified proteins in human kidney. *Am. J. Pathol.* **150**:603–614.
24. Lamb, N.J., Gutteridge, J.M., Baker, C., Evans, T.W., and Quinlan, G.J. 1999. Oxidative damage to proteins of bronchoalveolar lavage fluid in patients with acute respiratory distress syndrome: evidence for neutrophil-mediated hydroxylation, nitration, and chlorination. *Crit. Care Med.* **27**:1738–1744.
25. Reynolds, W.F., Chang, E., Douer, D., Ball, E.D., and Kanda, V. 1997. An allelic association implicates myeloperoxidase in the etiology of acute promyelocytic leukemia. *Blood.* **90**:2730–2737.
26. London, S.J., Lehman, T.A., and Taylor, J.A. 1998. Myeloperoxidase genetic polymorphism and lung cancer risk. *Cancer Res.* **57**:5001–5003.
27. Foster, C.B., et al. 1998. Host defense molecule polymorphisms influence the risk for immune-mediated complications in chronic granulomatous disease. *J. Clin. Invest.* **102**:2146–2155.
28. Reynolds, W.F., et al. 1999. Myeloperoxidase polymorphism is associated with gender specific risk for Alzheimer's disease. *Exp. Neurol.* **155**:32–42.
29. Albrich, J.M., McCarthy, C.A., and Hurst, J.K. 1981. Biological reactivity of hypochlorous acid: implications for microbicidal mechanisms of leukocyte myeloperoxidase. *Proc. Natl. Acad. Sci. USA.* **78**:210–214.
30. Thomas, E.L., Jefferson, M.M., and Grisham, M.B. 1982. Myeloperoxidase-catalyzed incorporation of amines into proteins: role of hypochlorous acid and dichloramines. *Biochemistry.* **21**:6299–6308.
31. Weiss, S.J., Klein, R., Slivka, A., and Wei, M. 1982. Chlorination of taurine by human neutrophils. Evidence of hypochlorous acid generation. *J. Clin. Invest.* **70**:598–607.
32. Winterbourn, C.C., VandenBerg, J.J.M., Roitman, E., and Kuypers, F.A. 1992. Chlorohydrin formation from unsaturated fatty acids reacted with hypochlorous acid. *Arch. Biochem. Biophys.* **296**:547–555.
33. Heinecke, J.W., Li, W., Mueller, D.M., Bohrer, A., and Turk, J. 1994. Cholesterol chlorohydrin synthesis by the myeloperoxidase-hydrogen peroxide-chloride system: potential markers for lipoproteins oxidatively damaged by phagocytes. *Biochemistry.* **33**:10127–10136.
34. Hazen, S.L., Hsu, F.F., Duffin, K., and Heinecke, J.W. 1996. Molecular chlorine generated by the myeloperoxidase-hydrogen peroxide-chloride system of phagocytes converts low density lipoprotein cholesterol into a family of chlorinated sterols. *J. Biol. Chem.* **271**:23080–23088.
35. Domigan, N.M., Charlton, T.S., Duncan, M.W., Winterbourn, C.C., and Kettle, A.J. 1995. Chlorination of tyrosyl radical in peptides by myeloperoxidase and human neutrophils. *J. Biol. Chem.* **270**:1652–1658.
36. Hazen, S.L., Hsu, F.F., Mueller, D.M., Crowley, J.R., and Heinecke, J.W. 1996. Human neutrophils employ chlorine gas as an oxidant during phagocytosis. *J. Clin. Invest.* **98**:1283–1289.
37. Heinecke, J.W., Li, W., Daehnke, H.L., and Goldstein, J.A. 1993. Dityrosine, a specific marker of oxidation, is synthesized by the myeloperoxidase-hydrogen peroxide system of human neutrophils and macrophages. *J. Biol. Chem.* **268**:4069–4076.
38. Savenkova, M.I., Mueller, D.M., and Heinecke, J.W. 1994. Tyrosyl radical generated by myeloperoxidase is a physiological catalyst for initiation of lipid peroxidation in low density lipoprotein. *J. Biol. Chem.* **269**:20394–20401.
39. Heinecke, J.W., Li, W., Francis, G.A., and Goldstein, J.A. 1993. Tyrosyl radical generated by myeloperoxidase catalyzes the oxidative crosslinking of proteins. *J. Clin. Invest.* **91**:2866–2872.
40. Van der Vliet, A., Eiserich, J.P., Halliwell, B., and Cross, C.E. 1997. Formation of reactive nitrogen species during peroxidase-catalyzed oxidation of nitrite. A potential additional mechanism of nitric oxide-dependent toxicity. *J. Biol. Chem.* **272**:7617–7625.
41. Jiang, Q., and Hurst, J.K. 1997. Relative chlorinating, nitrating and oxidizing capabilities of neutrophil determined with phagocytosable probes. *J. Biol. Chem.* **272**:32767–32772.
42. Eiserich, J.P., et al. 1998. Formation of nitric oxide-derived inflammatory oxidants by myeloperoxidase in neutrophils. *Nature.* **391**:393–395.
43. Podrez, E.A., Schmitt, D., Hoff, H.F., and Hazen, S.L. 1999. Myeloperoxidase-generated reactive nitrogen species convert LDL into an atherogenic form in vitro. *J. Clin. Invest.* **103**:1547–1560.
44. Byun, J., Mueller, D.M., Fabjan, S., and Heinecke, J.W. 1999. Nitrogen dioxide radical generated by the myeloperoxidase-hydrogen peroxide-nitrite system promotes lipid peroxidation of low density lipoprotein. *FEBS Lett.* **455**:243–246.
45. Berliner, J.A., et al. 1995. Atherosclerosis: basic mechanisms. Oxidation,

inflammation and genetics. *Circulation.* **91**:2488–2496.

46. Lusis, A.J. 2000. Atherosclerosis. *Nature.* **40**:233–241.

47. Heinecke, J.W. 1998. Oxidants and antioxidants in the pathogenesis of atherosclerosis: implications for the oxidized low density lipoprotein hypothesis. *Atherosclerosis.* **141**:1–15.

48. Leeuwenburgh, C., et al. 1997. Mass spectrometric quantification of markers for protein oxidation by tyrosyl radical, copper, and hydroxyl radical in low density lipoprotein isolated from human atherosclerotic plaques. *J. Biol. Chem.* **272**:3520–3526.

49. Beckmann, J.S., et al. 1994. Extensive nitration of protein tyrosines in human atherosclerosis detected by immunohistochemistry. *Biol. Chem. Hoppe Seyler.* **375**:81–88.

50. Leeuewenburgh, C., et al. 1997. Reactive nitrogen intermediates promote low density lipoprotein oxidation in human atherosclerotic intima. *J. Biol. Chem.* **272**:1433–1436.

51. Hazell, L.J., and Stocker, R. 1993. Oxidation of low-density lipoprotein with hypochlorite causes transformation of the lipoprotein into a high-uptake form for macrophages. *Biochem. J.* **290**:165–172.

52. Hazell, L.J., van den Berg, J.J., and Stocker, R. 1994. Oxidation of low-density lipoprotein by hypochlorite causes aggregation that is mediated by modification of lysine residues rather than lipid oxidation. *Biochem. J.* **302**:297–304.

53. Podrez, E.A., et al. 2000. Macrophage scavenger receptor CD36 is the major receptor for LDL modified by monocyte-generated reactive nitrogen species. *J. Clin. Invest.* **105**:1095–1108.

54. Aratani, Y., et al. 1999. Severe impairment in early host defense against *Candida albicans* in mice deficient in myeloperoxidase. *Infect. Immun.* **67**:1828–1836.

55. Venturelli, D., Bittenbender, S., and Rovera, G. 1989. Sequence of the murine myeloperoxidase (MPO) gene. *Nucleic Acids Res.* **17**:7987–7988.

56. Johnson, K.R., et al. 1987. Characterization of cDNA clones for human myeloperoxidase: predicted amino acid sequence and evidence for multiple mRNA species. *Nucleic Acids Res.* **15**:2013–2028.

57. Kaplow, L.S. 1965. Simplified myeloperoxidase stain using benzidine dihydrochloride. *Blood.* **26**:215–219.

58. Mayo, L.A., and Curnutte, J.T. 1990. Kinetic microplate assay for superoxide production by neutrophils and other phagocytic cells. *Methods Enzymol.* **186**:567–575.

59. Kettle, A.J., and Winterbourne, C.C. 1994. Assays for the chlorination activity of myeloperoxidase. *Methods Enzymol.* **233**:502–512.

60. Heinecke, J.W., et al. 1998. Detecting oxidative modification of biomolecules with isotope dilution mass spectrometry: sensitive and quantitative assays for oxidized amino acids in proteins and tissues. *Methods Enzymol.* **300**:124–144.

61. Lehrer, R.I., and Cline, M.J. 1969. Interaction of *Candida Albicans* with human leukocytes and serum. *J. Bacteriol.* **98**:996–1004.

62. Lehrer, R.I. 1970. Measurement of candidacidal activity of specific leukocyte types in mixed cell populations. I. Normal, myeloperoxidase-deficient, and chronic granulomatous disease neutrophils. *Infect. Immun.* **2**:42–47.

63. Wakeland, E., Morel, L., Achey, K., Yui, M., and Longmate, J. 1997. Speed congenics: a classic technique moves into the fast lane (relatively speaking). *Immunol. Today.* **18**:472–477.

64. Linton, M.F., Atkinson, J.B., and Fazio, S. 1995. Prevention of atherosclerosis in apolipoprotein E-deficient mice by bone marrow transplantation. *Science.* **267**:1034–1037.

65. Navab, M., et al. 1997. Mildly oxidized LDL induces apolipoprotein J/paraoxonase ratio. *J. Clin. Invest.* **99**:2005–2019.

66. Tangirala, R.J., Rubin, E.M., and Palinski, W. 1995. Quantitation of atherosclerosis in murine models: correlation between lesions in the aortic origin and in the entire aorta, and differences in the extent of lesions between sexes in LDL receptor-deficient and apolipoprotein E-deficient mice. *J. Lipid Res.* **36**:2320–2328.

67. Qiao, J.H., et al. 1994. Pathology of atheromatous lesions in inbred and genetically engineered mice: genetic determination of arterial calcification. *Arterioscler. Thromb.* **14**:1480–1497.

68. Fenna, R., Zeng, J., and Davey, C. 1995. Structure of the green heme in myeloperoxidase. *Arch. Biochem. Biophys.* **316**:653–656.

69. Odds, F.C. 1988. *Candida and candidosis.* Bailliere Tindall. London, United Kingdom. 253–258.

70. Ishibashi, S., Goldstein, J.L., Brown, M.S., Herz, J., and Burns, D.K. 1994. Massive xanthomatosis and atherosclerosis in cholesterol-fed low density lipoprotein receptor-negative mice. *J. Clin. Invest.* **93**:1885–1893.

71. Boisvert, W.A., Santiago, R., Curtiss, L.K., and Terkeltaub, R.A. 1998. A leukocyte homologue of the IL-8 receptor CXCR-2 mediates the accumulation of macrophages in atherosclerotic lesions of LDL receptor-deficient mice. *J. Clin. Invest.* **101**:353–363.

72. Babaev, V.R., et al. 1999. Macrophage lipoprotein lipase promotes foam cell formation and atherosclerosis in vivo. *J. Clin. Invest.* **103**:1697–1705.

73. Paigen, B., et al. 1987. Ath-1, a gene determining atherosclerosis susceptibility, and high density lipoprotein levels in mice. *Proc. Natl. Acad. Sci. USA.* **84**:3763–3767.

74. Clark, R.A., and Klebanoff, S.J. 1979. Chemotactic factor inactivation by the myeloperoxidase-hydrogen peroxide-halide system. An inflammatory control mechanism. *J. Clin. Invest.* **64**:913–920.

75. Weiss, S.J., Peppin, G., Ortiz, X., Ragsdale, C., and Test, S.T. 1985. Oxidative autoactivation of latent collagenase by human neutrophils. *Science.* **227**:1231–1233.

76. El Hag, A., and Clark, R.A. 1987. Immunosuppression by activated human neutrophils. Dependence on the myeloperoxidase system. *J. Immunol.* **139**:2406–2413.

77. Marcinkiewicz, J. 1997. Neutrophil chloramines: missing links between innate and acquired immunity. *Immun. Today.* **18**:577–580.

78. Francis, G.A., Mendez, A.J., Bierman, E.L., and Heinecke, J.W. 1993. Oxidative tyrosylation of high density lipoprotein by peroxidase enhances cholesterol removal from cultured fibroblasts and macrophage foam cells. *Proc. Natl. Acad. Sci. USA.* **90**:6631–6635.

79. Shern-Brewer, R., Satanam, N., Wetzstein, C., White-Whelkley, J., and Parthasarathy, S. 1998. Exercise and cardiovascular disease: a new perspective. *Arterio. Thromb. Vasc. Biol.* **18**:1181–1187.

80. Abu-Soud, H., and Hazen, S.L. 2000. Nitric oxide is a physiologic substrate for mammalian peroxidases. *J. Biol. Chem.* **275**:37524–37532.

81. Rausch, P.G., and Moore, T.G. 1975. Granule enzymes of polymorphonuclear neutrophils: a phylogenetic comparison. *Blood.* **46**:913–919.

82. Zhao, W.G., Lu, J.P., Regmi, A., and Austin, G.E. 1997. Identification and functional analysis of multiple murine myeloperoxidase (MPO) promoters and comparison with the human MPO promoter region. *Leukemia.* **11**:97–105.

83. Xie, Q.-W., and Nathan, C. 1992. *Biological oxidants: generation and injurious consequences.* C. Cochrane and M.J. Gimbrone, editors. Academic Press. San Diego, California, USA. 213–235.

84. Abu-Soud, H., and Hazen, S.L. 1999. Nitric oxide modulates the catalytic activity of myeloperoxidase. *J. Biol. Chem.* **275**:5425–5430.

85. Maeda, N., et al. 2000. Aortic wall damage in mice unable to synthesize ascorbic acid. *Proc. Natl. Acad. Sci. USA.* **97**:841–846.

86. Jandl, R.C., et al. 1978. Termination of the respiratory burst in human neutrophils. *J. Clin. Invest.* **61**:1176–1185.

87. Kirk, E.A., et al. 2000. Impaired superoxide production due to a deficiency in phagocyte NADPH oxidase fails to inhibit atherosclerosis in mice. *Arterio. Thromb. Vasc. Biol.* **20**:1529–1535.

88. Kubo, H., et al. 1996. Preservation of complement-induced lung injury in mice with deficiency of NADPH oxidase. *J. Clin. Invest.* **97**:2680–2684.